Published OnlineFirst November 2, 2017; DOI: 10.1158/2326-6066.CIR-17-0249

Research Article

Cancer Immunology Research

Intratumoral CD8$^+$ T-cell Apoptosis Is a Major Component of T-cell Dysfunction and Impedes Antitumor Immunity

Brendan L. Horton[1], Jason B. Williams[1], Alexandra Cabanov[2], Stefani Spranger[1], and Thomas F. Gajewski[1,3]

Abstract

Subsets of human tumors are infiltrated with tumor antigen–specific CD8$^+$ T cells [tumor-infiltrating lymphocytes (TILs)] despite tumor progression. These TILs are thought to be inactivated by the immunosuppressive tumor microenvironment, through the engagement of inhibitory receptors such as CTLA-4 and PD-1. However, antigen-specific CD8$^+$ TILs are not functionally inert but are undergoing activation *in situ*. Here, we show that antigen-specific CD8$^+$ TILs are actively proliferating, yet also undergo high rates of apoptosis, leading to a vicious cycle of activation and death that limits immune efficacy. Preventing CD8$^+$ TIL apoptosis by Bcl-x_L overexpression enabled accumulation and improved tumor control. Effective combination immunotherapy with an agonist 4-1BB mAb plus either CTLA-4 or PD-L1 neutralization led to a marked accumulation of specific CD8$^+$ TILs through decreased apoptosis rather than increased T-cell entry or proliferation. Our data suggest that antigen-driven apoptosis of CD8$^+$ TILs is a barrier to effective spontaneous antitumor immunity and should be considered as a critical factor in the development of cancer immunotherapies. *Cancer Immunol Res; 6(1); 14–24. ©2017 AACR.*

Introduction

Tumors from many different cancer types can be infiltrated by CD8$^+$ T cells [tumor-infiltrating lymphocytes (TILs; ref. 1)], and their presence has positive prognostic value (2). Despite their prognostic importance, most T cell–infiltrated tumors grow progressively. Evidence has suggested that TILs become functionally impaired through a multitude of immunosuppressive mechanisms within the tumor microenvironment, including engagement of the inhibitory receptor PD-1 by its major ligand PD-L1 (3), the activity of metabolic enzymes such as indoleamine-2,3-dioxygenase (3), and extrinsic suppression by FoxP3$^+$ regulatory T cells (Tregs) (3). However, we have found that antigen-specific TILs appear activated, produce IFNγ *in situ*, and retain cytolytic potential despite expression of PD-1, LAG-3, and other inhibitory receptors (4). These results indicate that TILs within progressing tumors may not be as functionally inert as once thought, and raise the question of why these TILs are not able to control progressing tumors.

Immunotherapy that targets T-cell inhibitory receptors PD-1 or CTLA-4 can lead to impressive tumor control in patients (5, 6). Data from mouse models and human cancer patients suggest that blockade of inhibitory receptors predominantly acts on the preexisting T-cell infiltrate residing in the tumor microenvironment at the time of treatment onset (7, 8). In mouse models, efficacy of anti–CTLA-4 and anti–PD-L1 combination therapies did not require new migration of T cells to the tumor from lymphoid tissues (7). Similarly, clinical studies demonstrated that patients with tumors infiltrated by CD8$^+$ T cells are much more likely to benefit from checkpoint blockade immunotherapy (8). The efficacy of treatment has been assumed to correlate with a proliferative burst in TILs (8). However, our data indicated that TILs are already proliferating *in situ* (4). This led us to hypothesize that other mechanisms might account for failed T cell–mediated tumor elimination at baseline, as well as improved tumor control in the context of immunotherapy.

To test these hypotheses, we utilized the B16.SIY murine melanoma model. B16.SIY is a transplantable melanoma cell line that was originally isolated from a spontaneous murine melanoma and then engineered to expresses the model antigen SIYRYYGL (SIY). B16.SIY will grow progressively when transplanted subcutaneously into wild-type (WT), syngeneic C57BL/6 mice (9). This system allows us to study the immune response against a progressing tumor. The SIY peptide is presented to CD8$^+$ T cells in the context of H2-K^b (10), which enables monitoring of SIY-specific T-cell responses in tumor-bearing hosts using IFNγ ELISPOT, as well as SIY-pentamer staining and flow cytometry. CD8$^+$ TILs in B16.SIY tumors express receptors that are targets for antibody-based immunotherapy, including PD-1, CTLA-4, and 4-1BB, allowing us to study how immunotherapy influences tumor antigen-specific T-cell responses (4).

In the current study, we found that antigen-specific TILs were not only undergoing continuous proliferation but also apoptosis within the tumor microenvironment. This cycle of activation and death restrained T-cell numbers within the

[1]Department of Pathology, University of Chicago, Chicago, Illinois. [2]The Committee on Immunology, University of Chicago, Chicago, Illinois. [3]Department of Medicine, Section of Hematology/Oncology, University of Chicago, Chicago, Illinois.

Note: Supplementary data for this article are available at Cancer Immunology Research Online (http://cancerimmunolres.aacrjournals.org/).

Corresponding Author: Thomas F. Gajewski, University of Chicago, 5841 S. Maryland Ave., MC2115, Chicago, IL 60637. Phone: 773-702-4601; Fax: 773-702-3701; E-mail: tgajewsk@medicine.bsd.uchicago.edu

doi: 10.1158/2326-6066.CIR-17-0249

Published OnlineFirst November 2, 2017; DOI: 10.1158/2326-6066.CIR-17-0249

tumor and led to inadequate tumor control. In contrast to progressor tumors, spontaneously rejecting tumors showed 5-fold higher numbers of SIY-specific TILs without evidence of apoptosis. Overexpressing the antiapoptotic molecule Bcl-x_L in T cells reduced TIL apoptosis and increased TIL accumulation in progressor tumors, and anti–4-1BB combination immunotherapies promoted tumor control by a mechanism associated with prevention of TIL apoptosis. Therefore, tumor antigen–specific TIL apoptosis appears to be a critical limiting factor of T-cell immunity against tumors.

Materials and Methods

Mice

C57BL/6 and Rag2$^{-/-}$ mice were from Taconic. Lck^{pr}–Bcl-x_L mice were a gift from Dr. M. Alegre (University of Chicago, Chicago, IL). Transgenic 2C TCR mice were bred in our facility (11). All mice were housed at University of Chicago in specific pathogen-free conditions in accordance with the NIH animal care guidelines. Autochthonous melanoma mice were described previously (11). All experiments were approved by the Institutional Animal Care and Use Committee at the University of Chicago and followed international guidelines.

Cell culture and inoculation

B16.F10, MC57, and 1969 cells were engineered to express SIYRYYGL, a peptide isolated from a random peptide library that binds H-2K^b. The resulting cell lines B16.SIY, MC57.SIY, and 1969.SIY, respectively, were cultured in DMEM with 10% FBS and penicillin and streptomycin, as described previously (4). Cells (2×10^6) were inoculated subcutaneously into the right flank of each animal.

Cells were cultured for one month after thawing. Cells were tested yearly for mycoplasma contamination using the HEK-Blue system (Invivogen). Our laboratory previously generated B16.SIY and 1969.SIY cell lines (4, 9). MC57.SIY cells were a gift from Dr. Hans Schreiber (University of Chicago; ref. 12). Cell lines were not reauthenticated or tested for cell line cross-contamination in the past year.

Antibody treatments

All therapeutic and depleting mAbs were purchased from Bio X Cell. Antibodies (100 μg) to 4-1BB (LOB.12.3), CTLA-4 (UC10-4F10-11), and PD-L1 (10F.9G2) were injected intraperitoneally 7 days after tumor inoculation. For tumor outgrowth, mAbs were given on days 7, 10, 13, and 16 after tumor inoculation. To deplete CD4-, CD8- or NK1.1-expressing cells, mAbs (250 μg) to CD4 (GK1.5), CD8 (2.43), NK1.1 (PK136) were given 24 hours before tumor inoculation, and then every 7 days.

FTY720 administration

FTY720 (5 μg/mouse, Enzo) was dissolved in DMSO and then diluted in PBS before administration daily by oral gavage.

Flow cytometry

Cells were analyzed on either a BD Fortessa or LSR-II cytometer. SIY-loaded pentamers were from ProImmune. The following antibodies were used in analyses: BD Biosciences: CD45 (30-F11), CD3 (145-2C11), CD4 (RM4-5), CD8 (53-6.7), bromodeoxyuridine (BrdU; Bu20a), Ki-67 (35/Ki-67), and active caspase-3 (C92-605); eBioscience: LAG-3 (C9B7W), 4-1BB (17B5); BioLegend: PD-1 (RMPI-30); Thermo Fisher Scientific: γH2AX (CR55T33). Fixable viability dyes were used to gate out dead cells and were purchased from eBioscience. Tumors, lymph nodes and spleens were dissociated through a 70 μm cell strainer to generate cell suspensions. Tumor suspensions were centrifuged over a Ficoll–Hypaque gradient to isolate live mononuclear cells. Cell suspensions were stained with antibodies in PBS containing 1% FBS for 20 minutes at room temperature. For intracellular antigens, cells were fixed and permeabilized in FoxP3 buffer (eBioscience) for 30 minutes at room temperature, washed, and stained with intracellular antibodies for 30 minutes at room temperature. For Annexin V staining, cells were first stained with extracellular antibodies and fixable viability dyes. Immediately before analysis, cells were stained using the Annexin V Staining Kit (BD Biosciences, catalog number 559763).

Adoptive transfer

Splenocytes were isolated from 2C or 2C Bcl-x_L mice, and red blood cells were lysed with Gey's solution. Cells were stimulated with plate-bound CD3 and CD28 antibodies for 4 to 6 days to generate activated effector cells. A total of 1×10^6 cells were then transferred intravenously to mice with 7-day established tumors.

BrdU administration

BrdU (0.8 mg, BD) was given intraperitoneally 24 hours before animal sacrifice. After staining extracellular antigens, cells were fixed and permeabilized with FoxP3 buffer (eBioscience) for 30 minutes at room temperature. Cells were resuspended in PBS with DNase I (300 μg/mL, Roche) at 37°C for 1 hour. Cells were subsequently stained with anti-BrdU antibody at room temperature for 30 minutes.

Gene expression profiling

The microarray data are available in the Gene Expression Omnibus database under accession no. GSE79919.

Statistical analysis

GraphPad Prism was used to compute all statistical tests. Data represent mean ± SEM. Mann–Whitney U, Kruskal–Wallis, and two-way ANOVA statistical tests were calculated in GraphPad Prism: *, $P < 0.05$; **, $P < 0.01$; ***, $P < 0.001$; ****, $P < 0.0001$.

Results

Tumor antigen–specific CD8$^+$ T cells proliferate in the tumor microenvironment

We previously found that antigen-specific TILs acquired a phenotype that included PD-1, LAG-3, and 4-1BB expression (4). Despite inhibitory receptor expression, however, these TILs proliferated within the tumor microenvironment (4). To rule out the possibility that TILs proliferated at early stages of tumor growth but lost proliferation upon persistent tumor antigen exposure, we examined TIL proliferation over time as tumor growth was progressing. To detect TIL proliferation, we pulsed mice bearing subcutaneous B16.SIY tumors with BrdU 24 hours before sacrifice at various time points (Fig. 1A). Although little BrdU was incorporated 7 days after tumor injection, we observed consistent BrdU incorporation by TILs 10 to 21 days after tumor injection. Incorporation of BrdU was significantly greater in the TILs than in the spleen, indicating that TILs were constantly

Published OnlineFirst November 2, 2017; DOI: 10.1158/2326-6066.CIR-17-0249

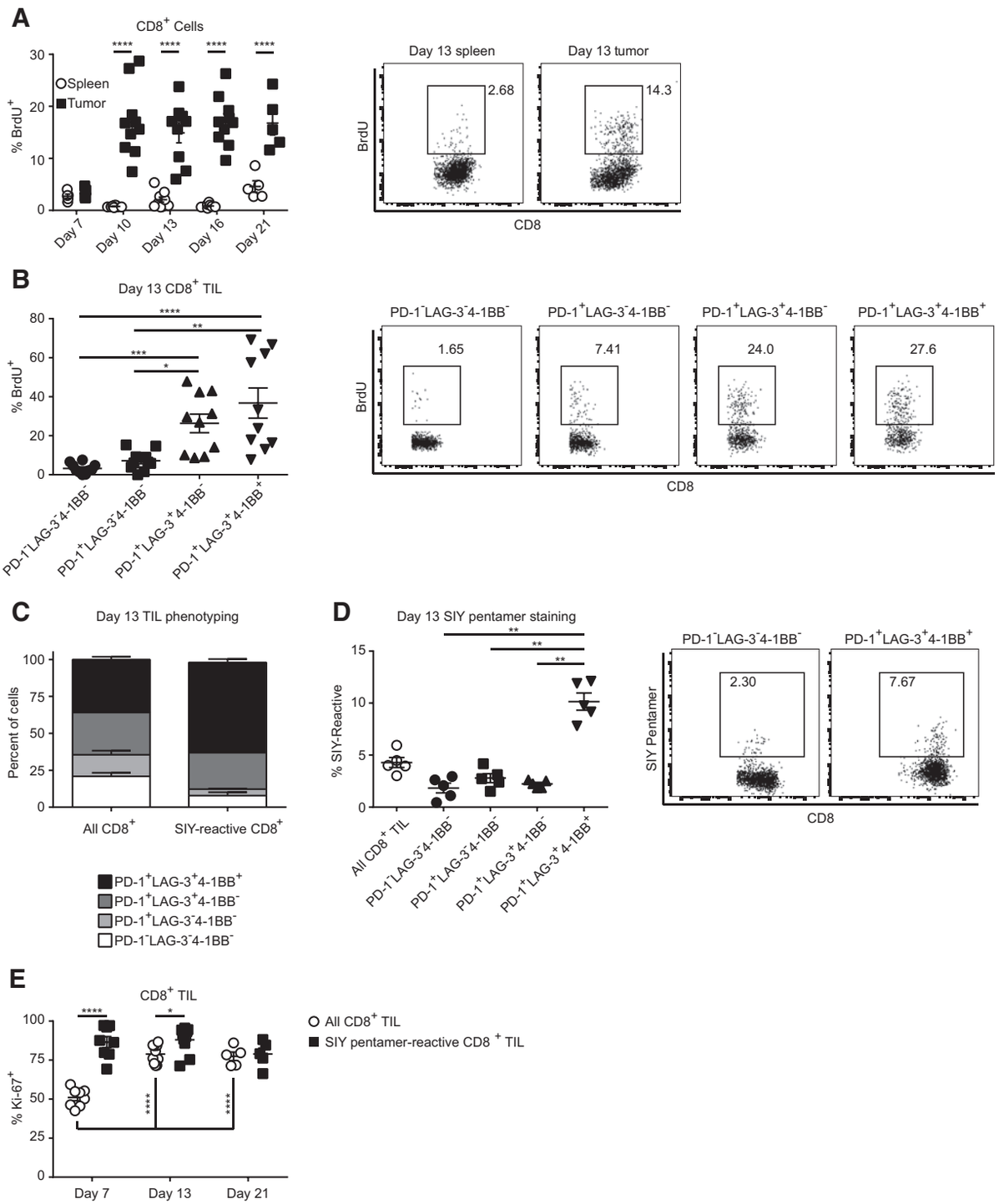

Figure 1.

CD8$^+$ T cells proliferate in the tumor microenvironment. **A,** C57BL/6 mice were injected subcutaneously with 2×10^6 B16.SIY tumor cells on day 0 and sacrificed at the indicated time points. One day prior to sacrifice, mice were injected intraperitoneally with BrdU (0.8 mg). Spleens and tumors of mice were analyzed via flow cytometry for BrdU incorporation in CD8$^+$ T cells. Day 7, $n = 5$; day 10, $n = 10$; day 13, $n = 10$; day 16, $n = 10$; day 21, $n = 5$. Data pooled from 3 independent experiments, two-way ANOVA. **B,** Analysis of TILs for the incorporation of BrdU on day 13, combined with phenotyping for the expression of PD-1, LAG-3, and 4-1BB. Data pooled from 2 independent experiments. One-way ANOVA, $n = 10$. **C** and **D,** TILs were stained with SIY pentamer and analyzed for the expression of PD-1, LAG-3, and 4-1BB on day 13 after tumor injection. Representative data from more than 3 independent experiments, $n = 5$, one-way ANOVA. **E,** Tumors of mice bearing B16.SIY tumors for 13 days were analyzed for SIY pentamer-reactive cells and Ki-67 expression via flow cytometry, day 7, $n = 8$; day 13, $n = 10$; day 21, $n = 5$. Data pooled from 3 independent experiments. Two-way ANOVA.

Published OnlineFirst November 2, 2017; DOI: 10.1158/2326-6066.CIR-17-0249

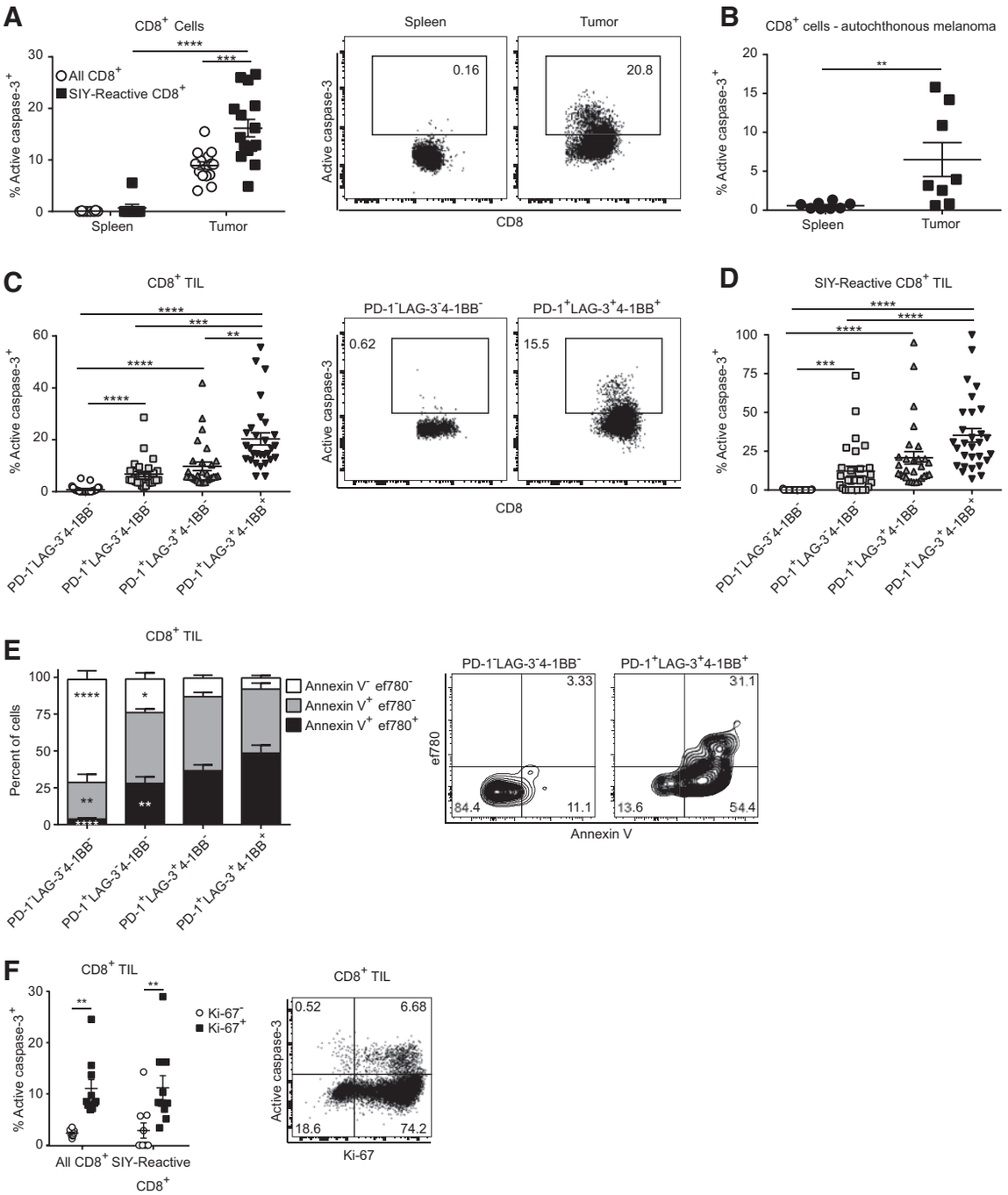

Figure 2.

CD8$^+$ T cells undergo apoptosis in the tumor microenvironment. **A,** CD8$^+$ cells from tumors and spleens of mice bearing B16.SIY tumors for 13 days were stained with SIY pentamer and analyzed for the presence of the active form of caspase-3 via flow cytometry. Data pooled from 3 independent experiments. Two-way ANOVA, $n = 15$. **B,** An autochthonous melanoma model driven by the melanocyte-specific, inducible expression of activated BRAF and deletion of PTEN was analyzed for the presence of active caspase-3 in CD8$^+$ T cells from spleens and melanomas via flow cytometry. Data pooled from 2 independent experiments. Mann–Whitney *U* test. **C,** TILs from B16.SIY tumor-bearing mice were analyzed for active caspase-3 as in **A** and for expression of PD-1, LAG-3, and 4-1BB via flow cytometry. Data pooled from 6 independent experiments. One-way ANOVA, $n = 29$. **D,** TILs were stained with SIY pentamer and analyzed as in **C**, $n = 29$. Data pooled from 6 independent experiments. **E,** TILs from B16.SIY were isolated and analyzed for the expression of PD-1, LAG-3, and 4-1BB, as well as binding to fluorescently labeled Annexin V and Fixable Viability Dye eFluor 780, $n = 10$. Data pooled from 2 independent experiments. Two-way ANOVA. The indicated statistical differences are compared with the PD-1$^+$LAG-3$^+$4-1BB$^+$ populations. **F,** TILs from mice bearing 13 day–established B16.SIY tumors were stained with SIY pentamer and analyzed for Ki-67 and active caspase-3 expression via flow cytometry, $n = 10$. Data pooled from 2 independent experiments, two-way ANOVA.

Published OnlineFirst November 2, 2017; DOI: 10.1158/2326-6066.CIR-17-0249

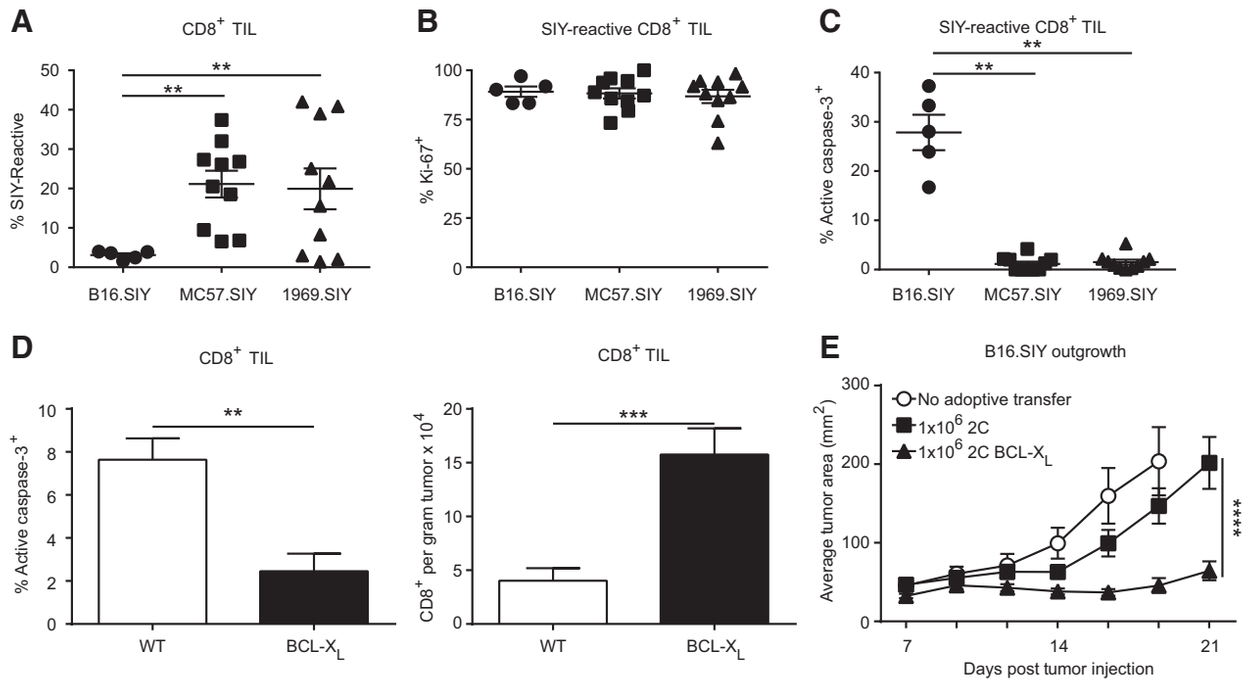

Figure 3.

Decreased TIL apoptosis leads to increased tumor control. **A,** C57BL/6 mice were injected with 2×10^6 B16.SIY, 2×10^6 MC57.SIY, or 2×10^6 1969.SIY cells on day 0. On day 7, mice were sacrificed and analyzed for SIY-reactive TILs via flow cytometry. One-way ANOVA, B16.SIY, $n = 5$; MC57.SIY and 1969.SIY, $n = 10$. **B,** Similar conditions to Ki-67 expression of SIY-reactive TILs are shown (**A**). One-way ANOVA; B16.SIY, $n = 5$; MC57.SIY and 1969.SIY, $n = 10$. **C,** As in **A**, the fraction of SIY-reactive cells with active caspase-3 is shown. One-way ANOVA; B16.SIY, $n = 5$; MC57.SIY and 1969.SIY, $n = 10$. All data in **A–C** is pooled from 2 independent experiments. **D,** Bcl-x_L or WT mice were injected with 2×10^6 B16.SIY cells on day 0. On day 13, mice were sacrificed and analyzed for active caspase-3 expression and to enumerate the number of TILs. Data pooled from 2 independent experiments. Mann–Whitney *U* test, $n = 9$. **E,** 2C or 2C Bcl-x_L splenocytes were activated *in vitro* with plate-bound antibodies to CD3 and CD28 to generate activated effector $CD8^+$ T cells. T cells (1×10^6) were transferred to mice bearing B16.SIY tumors on day 7 after tumor injection. No adoptive transfer, $n = 10$; 2C, $n = 10$; 2C Bcl-x_L, $n = 20$. Data pooled from 2 independent experiments, two-way ANOVA.

proliferating in the tumor microenvironment. To analyze antigen-specific TILs, we used K^b/SIY pentamers. Unfortunately, the BrdU staining interfered with the detection of pentamer-reactive cells. Expression of the surface receptors LAG-3 and 4-1BB identifies antigen-specific TILs (4); therefore, we phenotyped TILs for LAG-3 and 4-1BB while measuring BrdU incorporation (example phenotyping in Supplementary Fig. S1A). The most actively proliferating subpopulations of TILs expressed LAG-3 (Fig. 1B), suggesting that antigen-specific TILs were proliferating within the tumor microenvironment during tumor progression. LAG-3^+ populations remained the most proliferative subset of TILs over the course of tumor outgrowth (Supplementary Fig. S1B). Consistent with our previous finding that this surface phenotype enriches for antigen specificity (4), 80% to 90% of SIY-reactive TILs expressed LAG-3, or LAG-3, and 4-1BB (Fig. 1C), and conversely the PD-1^+LAG-3^+4-1BB$^+$ population was 3-fold more highly enriched for SIY-reactive TIL than the other phenotypic subsets (Fig. 1D). This phenotype was consistent over all time points analyzed (Supplementary Fig. S1C), indicating that antigen-specific TILs proliferate for the duration of tumor outgrowth. To confirm this directly, we analyzed Ki-67 expression as an alternative indicator of proliferation, as Ki-67 staining was compatible with SIY staining. Nearly all SIY-reactive TILs expressed Ki-67 at every time point analyzed (Fig. 1E). Despite this constant TIL proliferation, total TILs or SIY-reactive TILs did not significantly accumulate over the time points analyzed (Supplementary Fig. S1D and S1E). Therefore, some other process was restraining TIL accumulation despite constant proliferation.

Proliferating $CD8^+$ T cells undergo apoptosis in the tumor microenvironment

To investigate how TILs can constantly proliferate without accumulating, we asked whether these cells were simultaneously undergoing apoptosis within the tumor microenvironment. Caspase-3 is activated via cleavage during apoptosis, and effector T cells containing active caspase-3 are undergoing cell death (13, 14). Therefore, we utilized flow cytometry to detect intracellular active caspase-3. We found that at day 13 after tumor injection, a large fraction of TILs and SIY-reactive TILs contained active caspase-3 within the tumor but not in the spleen (Fig. 2A). Caspase-3 staining among TILs was consistent throughout tumor growth (Supplementary Fig. S2A). To test whether TILs apoptosed in nontransplantable tumor settings, we used an autochthonous, inducible B-Raf^{V600E}/PTEN$^{-/-}$ melanoma model. $CD8^+$ T cells within B-Raf^{V600E}/PTEN$^{-/-}$ melanomas also underwent apoptosis (Fig. 2B; ref. 11). Thus, $CD8^+$ T-cell apoptosis occurs specifically in the tumor microenvironment of tumors models with very different developmental origins and latency times.

Published OnlineFirst November 2, 2017; DOI: 10.1158/2326-6066.CIR-17-0249

We wanted to better understand the relationship between TIL surface phenotype, proliferation, and apoptosis. Phenotypic analysis revealed that TIL coexpressing LAG-3 and 4-1BB showed the highest rate of apoptosis (Fig. 2C), which suggested that antigen-specific TILs were simultaneously proliferating and dying. LAG-3$^+$4-1BB$^+$ TILs maintained the highest rates of apoptosis over time (Supplementary Fig. S2B). The rate of apoptosis of LAG-3$^+$4-1BB$^+$ cells was not significantly changed over the analyzed time points, indicating that even at fairly early times, LAG-3$^+$4-1BB$^+$ TILs underwent apoptosis. This suggested that the acquisition of this phenotype in the tumor environment was associated with high rates of proliferation and apoptosis. Direct measurement of active caspase-3 in SIY-reactive TILs revealed similar patterns of increased apoptosis in LAG-3$^+$4-1BB$^+$ cells (Fig. 2D; Supplementary Fig. S2B). Antigen-specific TILs were therefore undergoing both proliferation and apoptosis in the tumor microenvironment, and both proliferation and apoptosis correlated with LAG-3 and 4-1BB expression.

We also stained TILs with Annexin V and a cell-impermeable viability dye to measure different stages of apoptosis. The LAG-3$^+$4-1BB$^+$ population had decreased nonapoptotic, Annexin V$^-$ cells, and far more cells in late apoptosis (Fig. 2E), indicating that many of the LAG-3$^+$4-1BB$^+$ were in the final stages of cell death, thus confirming that the ultimate fate for these TILs was death.

Both proliferating and dying TILs were LAG-3$^+$4-1BB$^+$, suggesting that the same TILs were undergoing both proliferation and apoptosis. To directly confirm this, we measured active caspase-3 and Ki-67 expression in total TILs and SIY-reactive TILs. Active caspase-3 was highest among TILs that were Ki-67$^+$, directly indicating that apoptosis of proliferating cells was occurring (Fig. 2F). Antigen-specific CD8$^+$ TILs were therefore trapped in a cycle of proliferation and apoptosis that potentially limited TIL accumulation and antitumor immunity.

Prevention of TIL apoptosis leads to improved tumor control

To determine the relationship between apoptosis, accumulation of TILs, and immune-mediated tumor control, we studied TIL apoptosis in syngeneic tumor cell lines (MC57.SIY and 1969.SIY), which are spontaneously rejected by the adaptive immune system (15, 16). This allowed comparison of TIL apoptosis in progressing versus regressing tumors, to determine whether TIL apoptosis was specific to tumor progression. When compared with progressing B16.SIY tumors, a 4- to 5-fold expansion of SIY-reactive TILs was observed in MC57.SIY and 1969.SIY tumors (Fig. 3A). This expansion did not appear to be the result of changes in proliferation, as the Ki-67$^+$ fraction of T cells was similar in progressing versus regressing tumors (Fig. 3B). However, apoptosis was only observed among TILs from B16.SIY progressing tumors (Fig. 3C). We previously found that CD8$^+$ TILs in MC57.SIY and 1969.SIY tumors did not significantly express LAG-3 or 4-1BB (4). Less CD8$^+$ TIL apoptosis in regressing tumors was consistent with decreased LAG-3$^+$4-1BB$^+$ CD8$^+$ TILs in regressing tumors, as LAG-3$^+$4-1BB$^+$ CD8$^+$ TILs are the most apoptotic (Fig. 1C). These results indicate that spontaneous TIL apoptosis is a feature of progressing and not regressing tumors.

To modulate apoptosis in T cells, we used the Lck^{pr}-Bcl-x$_L$ mouse that overexpresses the antiapoptotic molecule Bcl-x$_L$ in T cells (Bcl-x$_L$ mice). Bcl-x$_L$ mice challenged with B16.SIY tumors had significantly reduced apoptosis of TILs, and an increase in the number of infiltrating TILs (Fig. 3D). Proliferation between TILs from WT and Bcl-x$_L$ mice was not different, indicating the increase of TILs was, indeed, correlated with a reduction in apoptosis (Supplementary Fig. S3A). However, these mice paradoxically had a reduced percentage of SIY-reactive TILs (Supplementary Fig. S2A), likely because T cells of multiple specificities were allowed to accumulate. To restrict Bcl-x$_L$ expression to tumor antigen–specific CD8$^+$ T cells, we crossed Bcl-x$_L$ mice to 2C TCR transgenic mice, the T cells from which recognize the SIY peptide in the context of K^b (2C Bcl-x$_L$ mice; ref. 17). Splenocytes from either 2C or 2C Bcl-x$_L$ mice were activated *in vitro* with CD3/CD28 antibodies to generate primed effector T cells, which were then transferred intravenously to mice bearing 7-day established B16.SIY tumors. Bcl-x$_L$ expression in 2C T cells resulted in significantly improved tumor control than WT 2C cells, indicating that inhibiting effector T-cell apoptosis is sufficient for more effective immune-mediated tumor destruction *in vivo* (Fig. 3E).

Anti–4-1BB plus checkpoint blockade therapy leads to tumor regression and decreased TIL apoptosis

Because many TILs undergoing apoptosis express 4-1BB (Fig. 2C), and agonist antibodies that induce 4-1BB signaling drive activation of NF-κB, a prosurvival transcription factor (18), we investigated whether engagement of 4-1BB could reduce TIL apoptosis and improve antitumor immunotherapy. Clinical trials are testing anti–4-1BB in combination with blockade of immune inhibitory receptors, so we focused on an agonist 4-1BB antibody with either CTLA-4 or PD-L1 blockade. These combinations led to enhanced tumor control of established B16.SIY tumors (Fig. 4A). Immunotherapy led to increased SIY-reactive CD8$^+$ T cells in tumor-draining lymph node, spleen, and within the tumor of treated mice (Fig. 4B). CD8$^+$ cells were required for rejection, as RAG2$^{-/-}$ animals had no response to immunotherapy, and depletion of CD8$^+$ cells, but not of CD4$^+$ or NK1.1$^+$ cells, abrogated the therapeutic effects (Supplementary Fig. S3A-D). Because we found SIY-reactive CD8$^+$ cell accumulation both in secondary lymphoid tissues and in the tumor, it was important to determine whether the trafficking of newly primed cells to the tumor was necessary for TIL accumulation and tumor regression. The trafficking of lymphocytes from lymph nodes is dependent on the receptor S1P1, whose action can be inhibited by the molecule FTY720. FTY720 treatment has been shown to effectively deplete circulating lymphocytes by preventing their ability to exit lymphoid tissues and enter back into circulation. Therefore, we treated B16.SIY tumor-bearing mice with FTY720 along with administration of anti–4-1BB combination immunotherapy. Daily FTY720 beginning on day 7 after tumor injection did not significantly impact tumor control (Fig. 4C), indicating that therapeutic efficacy was largely mediated by TILs already present within the tumor when immunotherapy began. FTY720 was confirmed to efficiently block trafficking of T cells into the blood (Fig. 4D). However, tumor-bearing mice treated with FTY720 and immunotherapy had no deficit in the numbers of SIY-reactive CD8$^+$ T cells within the tumor microenvironment compared with vehicle-treated mice receiving immunotherapy (Fig. 4E), indicating that TILs were expanding within the tumor site independently of cells expanding in the lymph nodes. Therefore, TIL accumulation was being driven by an intratumoral process.

Because trafficking from lymphoid tissues was not required for SIY-reactive TIL accumulation after immunotherapy, we reasoned that either increased proliferation or decreased apoptosis of

Published OnlineFirst November 2, 2017; DOI: 10.1158/2326-6066.CIR-17-0249

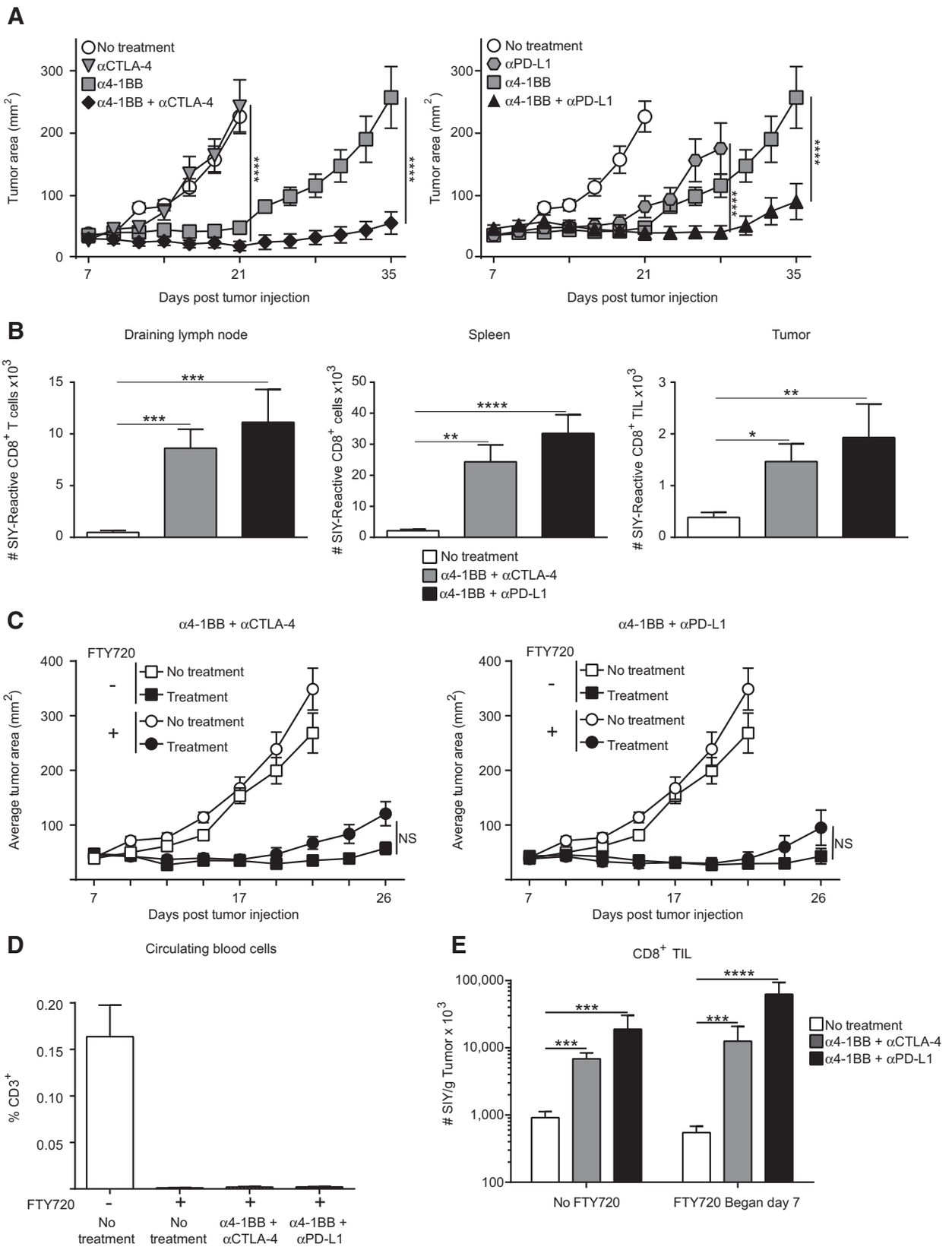

Published OnlineFirst November 2, 2017; DOI: 10.1158/2326-6066.CIR-17-0249

antigen-specific TILs was occurring. After immunotherapy, we found no difference in the proliferation of TILs (Fig. 5A). SIY-reactive TILs also showed no increase in Ki-67 expression (Fig. 5B). However, both the overall population of TILs and the SIY-reactive TIL subpopulation showed a significant reduction in active caspase-3 (Fig. 5C and D). Agonistic anti–4-1BB combination immunotherapy therefore appears to mediate tumor regression by boosting antigen-specific TIL accumulation via reduction of TIL apoptosis.

TILs have increased DNA damage

To better understand the mechanisms behind TIL apoptosis, we compared gene expression profiles from the PD-1$^+$LAG-3$^-$4-1BB$^-$ cell population to the PD-1$^+$LAG-3$^+$4-1BB$^+$ cell population (4). We chose these populations as their shared expression of PD-1 indicates they have recently seen their cognate antigen, but the PD-1$^+$LAG-3$^+$4-1BB$^+$ population is both much more proliferative and apoptotic. Using The Database for Annotation, Visualization and Integrated Discovery (DAVID) v6.8, we determined enriched gene ontology (GO) terms from 1,616 genes upregulated 2-fold or more in the PD-1$^+$LAG-3$^+$4-1BB$^+$ TILs. The two GO terms with the highest enrichment scores were associated with DNA damage (Fig. 6A). As DNA damage can lead to apoptosis, we measured DNA damage in TILs. Phosphorylated histone 2A, also known as γH2AX, is a marker of double-stranded DNA breaks readily detectable by robust flow cytometry antibodies. Using intracellular staining for γH2AX, we found significantly greater γH2AX staining in the total CD8$^+$ and SIY-reactive TIL, as compared with the spleen (Fig. 6B). γH2AX detection was the highest among the PD-1$^+$LAG-3$^+$4-1BB$^+$ TILs (Fig. 6C). Ki-67$^+$ TILs contained significantly more γH2AX than did Ki-67$^-$ TILs (Fig. 6D). However, γH2AX levels between CD8$^+$ splenocytes that were Ki-67$^+$ and Ki-67$^-$ were the same, indicating that proliferation itself was not sufficient to explain positive staining, but rather the accumulation of DNA damage was only found among proliferating T cells within the tumor microenvironment. We wanted to test more directly whether increased proliferation alone was responsible for increased detectable DNA damage, so we used 4-1BB combination immunotherapy to induce high proliferation in the CD8$^+$ T cells in peripheral lymphoid organs. Immunotherapy greatly increased the proliferation of these T cells, as measured by increased Ki-67 expression (Fig. 6E). However, γH2AX levels in CD8$^+$ T cells in the spleen and lymph nodes were not significantly increased after immunotherapy (Fig. 6F). Therefore, DNA damage in proliferating CD8$^+$ T cells occurs at high levels specifically within the tumor microenvironment, providing a potential cause of TIL apoptosis.

Discussion

We have previously found that TILs can retain IFNγ production and cytolytic potential, yet tumors progress nonetheless (4), leaving as an open question why TILs fail to eradicate the tumors in which they reside. CD8$^+$ TIL function and gene expression partially resemble exhausted CD8$^+$ T cells from chronic LCMV infections, raising the question of whether a unique type of dysfunction occurs in TILs that enables tumor progression (4). Our current data suggest that TILs undergo a cycle of activation and proliferation followed by death within the tumor microenvironment that leads to their failed expansion, allowing tumor outgrowth. When this cycle is interrupted, either through the enforced expression of the antiapoptotic factor Bcl-x_L or through anti–4-1BB combination immunotherapy, antigen-specific TIL accumulation is rescued and immune-mediated tumor control ensues. The fact that TILs are not as functionally inert as once thought is supported by other findings both in mouse models and with human tumors (19, 20). Our data suggest that rescuing TILs from apoptosis may be a vital strategy to increase immune-mediated tumor control, either to increase TIL number or to allow TILs to carry out their functions for a longer period of time. Whether additional functional improvements also contribute to better TIL efficacy after immunotherapy is not formally known, and it is possible additional functional alterations could also contribute to tumor regression. Although our results clearly demonstrate that TIL apoptosis represents one mechanism by which proliferating T cells fail to accumulate in the tumor microenvironment, it is not excluded that T-cell exit from the tumor may contribute. However, the LAG-3$^+$4-1BB$^+$ phenotype characteristic of proliferating antigen-specific CD8$^+$ T cells within the tumor microenvironment is not found in spleens or lymph nodes of tumor-bearing mice at any time point (4). Thus, if significant numbers of TILs do recirculate to other sites, they would need to change their surface phenotype rapidly, which seems unlikely.

We observed that simultaneous TIL proliferation and apoptosis occurred in progressively growing tumors, but not in tumors that underwent spontaneous rejection. In addition, TIL apoptosis was only seen in activated TILs expressing PD-1, with a higher percentage among those cells additionally expressing LAG-3 and 4-1BB. Apoptosis was not observed in the PD-1$^-$ TIL population, suggesting that the mere presence of T cells within the tumor microenvironment is not sufficient to result in T-cell death. Rather, those T cells undergoing antigen-driven activation *in situ* are those that show proliferation and apoptosis, and only under conditions when the tumor is not eliminated. These

Figure 4.

4-1BB combination immunotherapy leads to tumor regression and TIL accumulation through an intratumoral process. **A,** C57BL/6 mice were subcutaneously inoculated with B16.SIY cells (2×10^6). Tumors were established for 7 days; then, cohorts were treated with either single antibodies against 4-1BB, CTLA-4, or PD-L1, or combinations of anti–4-1BB + anti–CTLA-4, or anti–4-1BB + anti–PD-L1. Antibodies were given intraperitoneally on days 7, 10, 13, and 16 after tumor injection. Each mouse received 100 μg of each indicated antibody at each time point, $n = 10$ mice per cohort. Data pooled from 2 independent experiments, two-way ANOVA. **B,** Combination immunotherapy was given as in **A**, but mice were sacrificed on day 13 and tumor-draining lymph nodes, spleens, and tumors were analyzed for SIY-reactive CD8$^+$ T cells via flow cytometry. Data pooled from 2 independent experiments. One-way ANOVA, $n = 10$. **C,** C57BL/6 mice were injected subcutaneously with B16.SIY cells (2×10^6). Tumors were established for 7 days, at which point daily oral administration of FTY720 was begun. Mice received anti–4-1BB (100 μg) + anti–CTLA-4 (100 μg) or anti–4-1BB (100 μg) + anti–PD-L1 (100 μg) intraperitoneally on days 7, 10, 13, and 16 after tumor injection, $n = 10$. Data pooled from 2 independent experiments, two-way ANOVA. **D,** Blood from mice from **C** was analyzed at the endpoint of the experiment for circulating CD3$^+$ cells using flow cytometry. **E,** C57BL/6 mice were injected subcutaneously with B16.SIY cells (2×10^6). Tumors were established for 7 days, at which point daily oral administration of FTY720 was begun. Mice received anti–4-1BB (100 μg) + anti–CTLA-4 (100 μg) or anti–4-1BB (100 μg) + anti–PD-L1 (100 μg) intraperitoneally on days 7, and 10 after tumor injection and were analyzed on day 13. The accumulation of SIY-reactive TILs was analyzed with flow cytometry. Data pooled from 3 independent experiments, $n = 15$, one-way ANOVA.

Published OnlineFirst November 2, 2017; DOI: 10.1158/2326-6066.CIR-17-0249

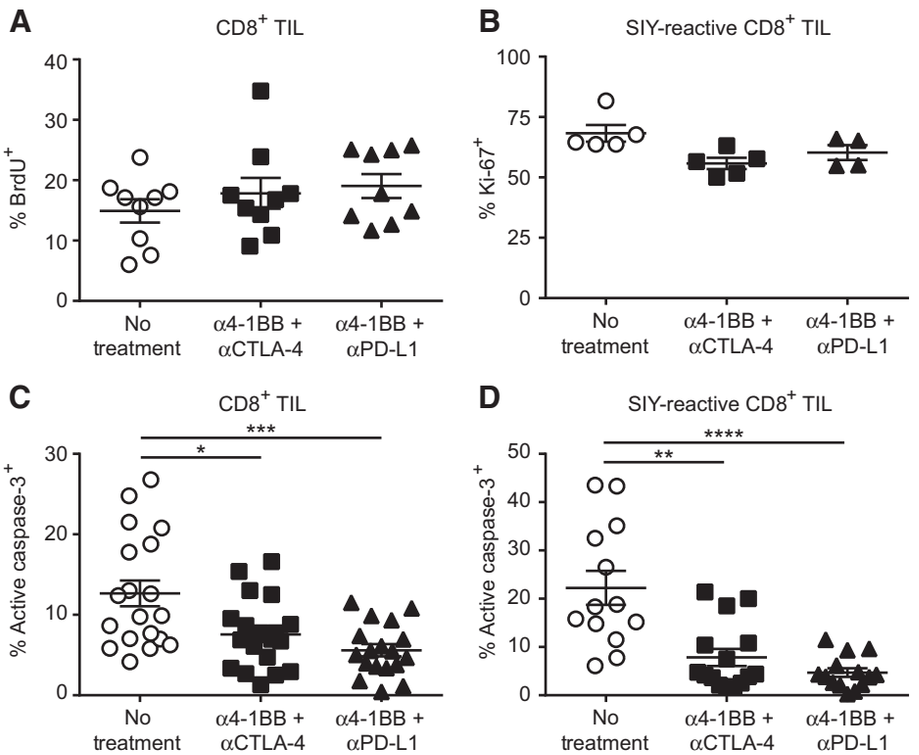

Figure 5.

Anti–4-1BB combination immunotherapy decreases TIL apoptosis. **A,** C57BL/6 mice were inoculated subcutaneously with 2×10^6 B16.SIY cells and treated with immunotherapy on day 7 and day 10 after tumor cell injection. BrdU (0.8 mg/mouse) was administered intraperitoneally 24 hours before sacrifice of each cohort. On day 13 after tumor cell injection, the tumors were analyzed using flow cytometry to detect $CD8^+$ T cells with incorporated BrdU; $n = 9$. Data pooled from 2 independent experiments. **B,** As in **A**, but Ki-67 expression was analyzed via flow cytometry. No treatment, $n = 5$; anti–4-1BB + anti–CTLA-4, $n = 5$; anti–4-1BB + anti–PD-L1, $n = 4$. **C,** As in **A**, but TILs were analyzed for the presence of active capase-3 via flow cytometry, data pooled from 4 independent experiments. No treatment, $n = 19$; anti–4-1BB + anti–CTLA-4, $n = 20$; anti–4-1BB + anti–PD-L1, $n = 18$; one-way ANOVA. **D,** As in **A**, but TILs were analyzed for the presence of active capase-3 and SIY reactivity via flow cytometry. Data pooled from 3 independent experiments. No treatment, $n = 13$; anti–4-1BB + anti–CTLA-4, $n = 15$; anti–4-1BB + anti–PD-L1, $n = 14$; one-way ANOVA.

data suggest apoptosis results from an active process involving TCR engagement and is a critical component of T-cell dysfunction resulting from chronic antigen stimulation. The detailed biochemical mechanisms driving TIL apoptosis remain to be pursued in future studies, but our current data suggest that accumulated DNA damage in TILs may play a role. Such DNA damage could result from the reactive oxygen species known to be produced in the context of a growing cancer, or the hypoxia and tissue stress that characterize solid tumors (21, 22). This result is consistent with published data indicating that $p53^{-/-}$ T cells are better able to control tumors upon adoptive transfer *in vivo* (23).

Our experiments with FTY720 indicate that major antitumor effects of anti–4-1BB combination immunotherapy can be exerted on the TILs present at baseline. This was the case despite the marked increase in tumor antigen–specific T cells in the tumor-draining lymph nodes in treated mice. These results suggest that 4-1BB expressed on TILs may be targeted directly by agonist 4-1BB immunotherapy. These data are also consistent with previous observations from both mouse and human studies that a preexisting T-cell infiltrate is associated with an increased likelihood of response to immunotherapy (7, 8). Thus, therapeutic blockade of inhibitory signals or enhancement of costimulatory signals may both act predominantly on tumor-infiltrating $CD8^+$ cells for the immediate therapeutic effect observed.

The effects of costimulation in the tumor microenvironment are relatively understudied, but are quickly becoming of interest. Costimulation through CD28 signaling is required for anti–PD-1 efficacy (24, 25). Blockade of CD28 inhibited the T-cell proliferation that normally occurred after PD-1 blockade (25). T cell–expressed ICOS is also necessary for the optimal effects of anti–CTLA-4–based immunotherapy (26). In our current study, we show that the delivery of additional costimulation signals through an agonist 4-1BB antibody increased the efficacy of PD-L1 or CTLA-4 blockade. However, 4-1BB combination immunotherapy did not increase the proliferation of TILs, but rather reduced TIL apoptosis. This is in line with previous findings that show that 4-1BB improves the survival of $CD8^+$ T cells in various other model systems (27–29). A prosurvival role of 4-1BB is also supported by studies demonstrating increased persistence of CAR T cells that include a 4-1BB signaling domain (30). As a member of the TNFR superfamily, it is conceivable that 4-1BB ligation mediates enhanced TIL survival through the NF-κB pathway, which is critical for T cell–mediated tumor control *in vivo* (15, 31).

Published OnlineFirst November 2, 2017; DOI: 10.1158/2326-6066.CIR-17-0249

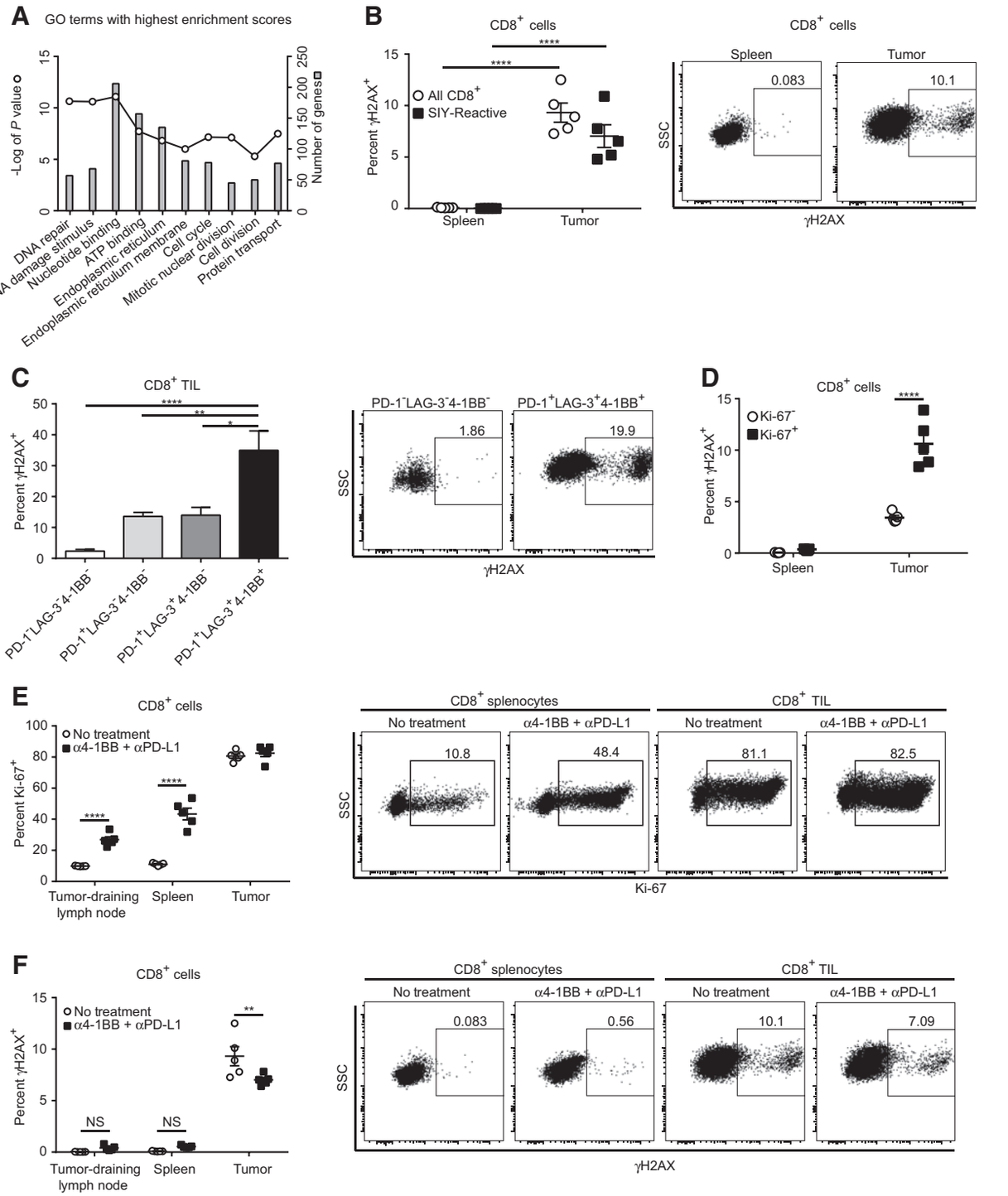

Figure 6.

TILs have increased DNA damage. **A,** Depicted are the top 10 enriched GO terms identified by DAVID from genes upregulated in PD-1$^+$LAG-3$^+$4-1BB$^+$ TILs compared with PD-1$^+$LAG-3$^-$4-1BB$^-$ TILs, the −log(*P* value) of each, and the number of genes from the upregulated genes that were included the each GO term. **B,** Day 13 CD8$^+$ cells from the spleens and tumors of mice were analyzed for γH2AX; $n = 5$, two-way ANOVA. **C,** TILs from day 13 tumors were analyzed for expression of PD-1, LAG-3, 4-1BB, and γH2AX; $n = 10$, one-way ANOVA. Data pooled from 2 independent experiments. **D,** Day 13 CD8$^+$ cells were analyzed for expression of Ki-67 and γH2AX; $n = 5$, two-way ANOVA. **E,** C57BL/6 mice were injected subcutaneously with B16.SIY cells (2×10^6) on day 0. On days 7 and 10, mice were treated with 100 μg anti–4-1BB plus 100 μg anti–PD-L1. On day 13, CD8$^+$ cells were analyzed for expression of Ki-67; $n = 5$, two-way ANOVA. **F,** The same CD8$^+$ cells from **E** were also analyzed for γH2AX; $n = 5$, two-way ANOVA.

Disclosure of Potential Conflicts of Interest

No potential conflicts of interest were disclosed.

Authors' Contributions

Conception and design: B.L. Horton, J.B. Williams, S. Spranger, T.F. Gajewski
Development of methodology: B.L. Horton, J.B. Williams, S. Spranger, T.F. Gajewski
Acquisition of data (provided animals, acquired and managed patients, provided facilities, etc.): B.L. Horton, J.B. Williams, A. Cabanov
Analysis and interpretation of data (e.g., statistical analysis, biostatistics, computational analysis): B.L. Horton, J.B. Williams, S. Spranger, A. Cabanov, T.F. Gajewski
Writing, review, and/or revision of the manuscript: B.L. Horton, S. Spranger, T.F. Gajewski
Administrative, technical, or material support (i.e., reporting or organizing data, constructing databases): B.L. Horton, J.B. Williams, T.F. Gajewski
Study supervision: T.F. Gajewski
Other: A. Cabanov

Acknowledgments

This work was supported by R35CA210098 from the NCI. B.L. Horton was funded by Cancer Biology Training Grant T32-CA09594. The flow cytometry core facility at the University of Chicago was funded by Cancer Center Support Grant (P30CA014599).

We would like to acknowledge Drs. Anita Chong, Maria-Luisa Alegre, and Justin Kline for insightful comments about this study.

The costs of publication of this article were defrayed in part by the payment of page charges. This article must therefore be hereby marked *advertisement* in accordance with 18 U.S.C. Section 1734 solely to indicate this fact.

Received May 18, 2017; revised September 5, 2017; accepted October 27, 2017; published OnlineFirst November 2, 2017.

References

1. Spranger S, Luke JJ, Bao R, Zha Y, Hernandez KM, Li Y, et al. Density of immunogenic antigens does not explain the presence or absence of the T-cell-inflamed tumor microenvironment in melanoma. Proc Natl Acad Sci USA 2016;113:E7759–68.
2. Fridman WH, Pages F, Sautes-Fridman C, Galon J. The immune contexture in human tumours: impact on clinical outcome. Nat Rev Cancer 2012; 12:298–306.
3. Gajewski TF, Schreiber H, Fu YX. Innate and adaptive immune cells in the tumor microenvironment. Nat Immunol 2013;14:1014–22.
4. Williams JB, Horton BL, Zheng Y, Duan Y, Powell JD, Gajewski TF. The EGR2 targets LAG-3 and 4-1BB describe and regulate dysfunctional antigen-specific CD8+ T cells in the tumor microenvironment. J Exp Med 2017;214:381–400.
5. Topalian SL, Hodi FS, Brahmer JR, Gettinger SN, Smith DC, McDermott DF, et al. Safety, activity, and immune correlates of anti-PD-1 antibody in cancer. N Eng J Med 2012;366:2443–54.
6. Larkin J, Chiarion-Sileni V, Gonzalez R, Grob JJ, Cowey CL, Lao CD, et al. Combined nivolumab and ipilimumab or monotherapy in untreated melanoma. N Eng J Med 2015;373:23–34.
7. Spranger S, Koblish HK, Horton B, Scherle PA, Newton R, Gajewski TF. Mechanism of tumor rejection with doublets of CTLA-4, PD-1/PD-L1, or IDO blockade involves restored IL-2 production and proliferation of CD8 (+) T cells directly within the tumor microenvironment. J Immunother Cancer 2014;2:3.
8. Tumeh PC, Harview CL, Yearley JH, Shintaku IP, Taylor EJ, Robert L, et al. PD-1 blockade induces responses by inhibiting adaptive immune resistance. Nature 2014;515:568–71.
9. Kline J, Brown IE, Zha YY, Blank C, Strickler J, Wouters H, et al. Homeostatic proliferation plus regulatory T-cell depletion promotes potent rejection of B16 melanoma. Clin Cancer Res 2008;14:3156–67.
10. Udaka K, Wiesmuller KH, Kienle S, Jung G, Walden P. Self-MHC-restricted peptides recognized by an alloreactive T lymphocyte clone. J Immunol 1996;157:670–8.
11. Spranger S, Bao R, Gajewski TF. Melanoma-intrinsic beta-catenin signalling prevents anti-tumour immunity. Nature 2015;523:231–5.
12. Spiotto MT, Yu P, Rowley DA, Nishimura MI, Meredith SC, Gajewski TF, et al. Increasing tumor antigen expression overcomes "ignorance" to solid tumors via crosspresentation by bone marrow-derived stromal cells. Immunity 2002;17:737–47.
13. Martin SJ, Amarante-Mendes GP, Shi L, Chuang TH, Casiano CA, O'Brien GA, et al. The cytotoxic cell protease granzyme B initiates apoptosis in a cell-free system by proteolytic processing and activation of the ICE/CED-3 family protease, CPP32, via a novel two-step mechanism. EMBO J 1996;15:2407–16.
14. Garrod KR, Moreau HD, Garcia Z, Lemaitre F, Bouvier I, Albert ML, et al. Dissecting T cell contraction *in vivo* using a genetically encoded reporter of apoptosis. Cell Rep 2012;2:1438–47.
15. Barnes SE, Wang Y, Chen L, Molinero LL, Gajewski TF, Evaristo C, et al. T cell-NF-kappaB activation is required for tumor control in vivo. J Immunother Cancer 2015;3:1.
16. Woo SR, Fuertes MB, Corrales L, Spranger S, Furdyna MJ, Leung MY, et al. STING-dependent cytosolic DNA sensing mediates innate immune recognition of immunogenic tumors. Immunity 2014;41:830–42.
17. Zhang L, Chen X, Liu X, Kline DE, Teague RM, Gajewski TF, et al. CD40 ligation reverses T cell tolerance in acute myeloid leukemia. J Clin Invest 2013;123:1999–2010.
18. Martinez-Forero I, Azpilikueta A, Bolanos-Mateo E, Nistal-Villan E, Palazon A, Teijeira A, et al. T cell costimulation with anti-CD137 monoclonal antibodies is mediated by K63-polyubiquitin-dependent signals from endosomes. J Immunol 2013;190:6694–706.
19. Boldajipour B, Nelson A, Krummel MF. Tumor-infiltrating lymphocytes are dynamically desensitized to antigen but are maintained by homeostatic cytokine. JCI Insight 2016;1:e89289.
20. Daud AI, Loo K, Pauli ML, Sanchez-Rodriguez R, Sandoval PM, Taravati K, et al. Tumor immune profiling predicts response to anti-PD-1 therapy in human melanoma. J Clin Invest 2016;126:3447–52.
21. Kondoh M, Ohga N, Akiyama K, Hida Y, Maishi N, Towfik AM, et al. Hypoxia-induced reactive oxygen species cause chromosomal abnormalities in endothelial cells in the tumor microenvironment. PLoS One 2013;8:e80349.
22. Klein TJ, Glazer PM. The tumor microenvironment and DNA repair. Semin Rad Oncol 2010;20:282–7.
23. Banerjee A, Thyagarajan K, Chatterjee S, Chakraborty P, Kesarwani P, Soloshchenko M, et al. Lack of p53 augments antitumor functions in cytolytic T cells. Cancer Res 2016;76:5229–40.
24. Hui E, Cheung J, Zhu J, Su X, Taylor MJ, Wallweber HA, et al. T cell costimulatory receptor CD28 is a primary target for PD-1-mediated inhibition. Science 2017;355:1428–33.
25. Kamphorst AO, Wieland A, Nasti T, Yang S, Zhang R, Barber DL, et al. Rescue of exhausted CD8 T cells by PD-1-targeted therapies is CD28-dependent. Science 2017;355:1423–27.
26. Fan X, Quezada SA, Sepulveda MA, Sharma P, Allison JP. Engagement of the ICOS pathway markedly enhances efficacy of CTLA-4 blockade in cancer immunotherapy. J Exp Med 2014;211:715–25.
27. Hernandez-Chacon JA, Li Y, Wu RC, Bernatchez C, Wang Y, Weber JS, et al. Costimulation through the CD137/4-1BB pathway protects human melanoma tumor-infiltrating lymphocytes from activation-induced cell death and enhances antitumor effector function. J Immunother 2011;34: 236–50.
28. Takahashi C, Mittler RS, Vella AT. Cutting edge: 4-1BB is a bona fide CD8 T cell survival signal. J Immunol 1999;162:5037–40.
29. Weigelin B, Bolanos E, Teijeira A, Martinez-Forero I, Labiano S, Azpilikueta A, et al. Focusing and sustaining the antitumor CTL effector killer response by agonist anti-CD137 mAb. Proc Natl Acad Sci USA 2015;112:7551–6.
30. Long AH, Haso WM, Shern JF, Wanhainen KM, Murgai M, Ingaramo M, et al. 4-1BB costimulation ameliorates T cell exhaustion induced by tonic signaling of chimeric antigen receptors. Nat Med 2015;21:581–90.
31. Evaristo C, Spranger S, Barnes SE, Miller ML, Molinero LL, Locke FL, et al. Cutting edge: engineering active IKKbeta in T cells drives tumor rejection. J Immunol 2016;196:2933–8.

Published OnlineFirst November 2, 2017; DOI: 10.1158/2326-6066.CIR-17-0249

Cancer Immunology Research

Intratumoral CD8$^+$ T-cell Apoptosis Is a Major Component of T-cell Dysfunction and Impedes Antitumor Immunity

Brendan L. Horton, Jason B. Williams, Alexandra Cabanov, et al.

Cancer Immunol Res 2018;6:14-24. Published OnlineFirst November 2, 2017.